

# Bone Architecture: Collagen Structure and Calcium/Phosphorus Maps

Margaret Tzaphlidou

Received: 25 October 2007 / Accepted: 9 September 2008 /  
Published online: 15 October 2008  
© Springer Science + Business Media B.V. 2008

**Abstract** Bone collagen structure in normal and pathological tissues is presented using techniques of thin section transmission electron microscopy and morphometry. In pathological tissue, deviations from normal fine structure are reflected in abnormal arrangements of collagen fibrils and abnormalities in fibril diameter. The relationships between these bone structural changes and the skeletal calcium/phosphorus ratio are discussed. Calcium/phosphorus ratio is measured by X-ray absorptiometry and computed microtomography.

**Keywords** Bone · Collagen · Electron microscopy · Morphometry · X-ray absorptiometry · Synchrotron radiation microtomography · Calcium/phosphorus ratio

## 1 Introduction

Bone is highly hierarchical in structure [1, 2], and therefore, any study of its structure and properties must investigate the tissue at several levels of organization in order to gain a complete understanding of the influence of structure and composition on these properties.

The extracellular matrix, and especially connective tissue with its collagen, plays an important role in the force transmission and bone structure maintenance. The turnover of the matrix is influenced by physical activity, and both collagen synthesis and degrading metalloprotease enzymes increase with mechanical loading [3]. In bone, the formation and mineralization of the extracellular matrix structure is a complex process highly dependent on intermolecular interactions [4]. The most abundant matrix protein and one of the major constituents implicated in mineralization is type I collagen [5–7], although there is a considerable number of minor collagen types present [8].

---

M. Tzaphlidou (✉)  
Department of Medical Physics, Medical School, Ioannina University, 45110, Ioannina, Greece  
e-mail: mtzaphli@uoi.gr

Structure and microarchitecture are determinant aspects of bone strength and essential elements for the assessment of bone mechanical properties. Microarchitecture seems to be a determinant of bone fragility independent of bone density as well as important in order to understand the mechanisms of bone fragility [9]. Among other factors, microarchitecture is affected by loading. Loading also affects bone mass and size, and it is therefore important for the maintenance of bone strength during normal aging; in combination with exercise, it plays an important role in the prevention of osteoporotic fractures [10].

Reliable measures of the dynamic and static strength of the skeleton are required for the understanding and management of clinical osteoporosis. Measurement of bone mineral content by DEXA or MRI is generally accepted as an appropriate estimate of bone strength. The major high Z mineral components in bone (ICRU-44, 1989) are Ca and P and may provide a sensitive measure of bone mineral changes. Monitoring these elements could add to our understanding of the changes that occur in normal and diseased bone. Since bone is a biomaterial that is structurally adapted to different functions and loading situations, the exact composition is expected to depend on sex, age, type, bone site, and disease [11]. Conventional DEXA is unable to distinguish changes in the amounts of Ca and P in biological apatite. Furthermore, these changes do not necessarily go hand-in-hand; a decrease in bone density due to a decrease in either Ca or P or to dissimilar decreases in both cannot be monitored. Thus, the determination of the Ca/P ratio could lead to a greater understanding of the role played by these elements.

## 2 Normal/Abnormal Bone Collagen

Well-understood differences between normal and abnormal bone include lower bone mineral density and thinner bone struts in the abnormal bone. However, relatively few studies have analyzed the structure of normal compared with abnormal bone, leaving many unanswered questions concerning the quality of the bone in the abnormal tissue.

Bone quality depends on a number of parameters. Such parameters include micro- and macro-architecture, bone remodeling rate, microdamage, apoptosis of bone cellular populations, and properties of the bone matrix, such as size of crystals, mineralization, collagen structure, and cross-linking.

In bone, collagen represents more than 90% of the organic matrix. In abnormal bone, collagen quality is affected [12–14]. There is evidence from the work of Bailey et al. [12] that significant changes occur in the posttranslational modifications which could seriously affect the properties of the fibrils; in particular, an overhydroxylation as well as an alteration and reduction of cross-linking related to the increase in bone fragility were detected. Also, other workers [15] related the extent of change in hydroxylation to the trabecular volume and density of bone, although the relationship was unclear.

In contrast, Bank et al. [16] pointed out that the brittleness of bone in patients with osteogenesis imperfecta is not caused by a disorganized intrafibrillar collagen packing and/or loss of cross-links. Other evidence [14] suggests that, in several types of osteogenesis imperfecta, triple helix formation is impaired, the predominant type of bone collagen, type I, is posttranslationally overmodified, and extracellular secretion is markedly reduced. The conclusion by Prockop et al. [17] that most variants of osteogenesis imperfecta are caused by mutations in the structural genes for type I procollagen seems to have broad implications for other diseases that affect connective tissue, such as osteoarthritis and osteoporosis. In

normal and osteoporotic human bone, no differences were observed [18] in the length and thickness of apatite crystals in collagen fibrils at the nanostructural level.

## 2.1 Fibril Architecture and Diameter

Collagen type I is typical fibrillar collagen that consists largely of rectilinear arrays of collagen fibrils [19]. In bone, trabecular and cortical, although fibrils maintain their regular parallel arrangement (Fig. 1a, c), they are not uniformly distributed as in other tissues such as skin. In addition, in bone, the collagen matrix is very dense. These observations have been found in various experimental species: rabbits [20], rats [13], and mice [21].

In a number of studies, defective collagen fibril formation and architecture upon abnormalities were observed. Osteoporosis is characterized by unusual architectural and compositional features [22]. Results derived from osteoporosis induced either by inflammation (IMO) [20, 23] or by ovariectomy [13] suggest that the overall bone collagen fibril architecture is dramatically affected; in both bone types (trabecular, cortical), collagen fibril architecture has a random arrangement (Fig. 1b, d) compared with normal (Fig. 1a, c).

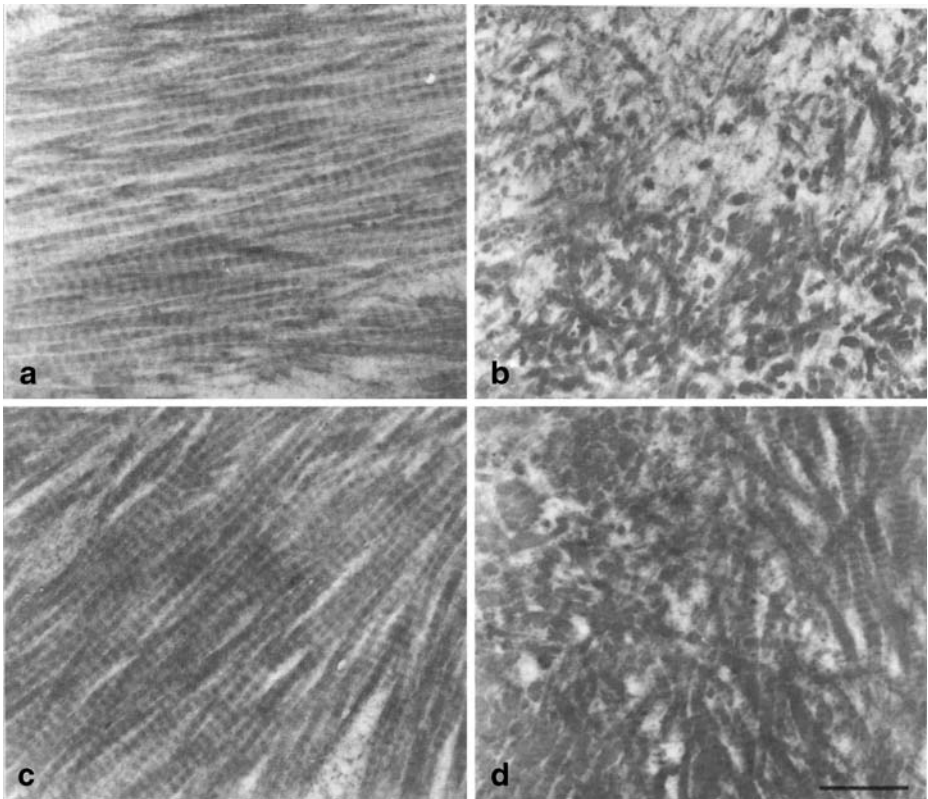


**Fig. 1** Electron micrographs of rat collagen: **a, b** trabecular, **c, d** cortical bone fibrils, from normal animals (**a, c**) and from ovariectomized rats (**b, d**). The latter fibrils have an irregular arrangement in contrast to controls. *Bar* = 0.5  $\mu\text{m}$

These morphological observations of the electron-microscopic images of collagen bundles in control and treated animals were based on a very large number of sections from different blocks and animals.

The collagen fibril diameter has been regarded as the most important factor related to biomechanical strength of tissues [24–26]. A number of factors have been implicated in the regulation of tissue collagen fibril diameter. Among them, the different collagen types that are included in a variety of tissues are mostly responsible for the variation in collagen fibril diameter seen in various tissues [19]. In tissues, thin-sectioned fibrils cut transversely allow their diameters to be measured. In transverse sections (cross-sections) from healthy material, where fibrils usually appear circular in outline, many tissues show a good uniformity in fibril diameters. Bone fibrils have a regular outline, and no fibrils with outline deviating from a circular profile are present. In addition, a uniform fibril diameter distribution is apparent. The diameter spread is not broad, with diameters ranging from 30 to 80 nm [8].

For bone collagen fibril diameter, among other factors, the kind of species and bone site may be important. In normal rear cortical tibia from rabbits, mean collagen fibril diameter differs significantly ( $p < 0.001$ ) than that deriving from rats or mice [8]. Furthermore, a significant difference ( $p < 0.001$ ) in mean fibril diameter from cortical femur or cortical tibia between rabbits and rats was found [27] demonstrating a dependence upon the kind of experimental animal. Table 1 compares these mean diameter values. Also, in these subjects, statistically significant differences ( $0.001 < p < 0.04$ ) were detected between different bone sites, e.g., between front and rear tibia, as well as between rear tibia and femur, demonstrating a dependence upon bone site. It is worth noting that no statistically significant differences in mean collagen fibril diameter values, for the same bone site, between cortical and trabecular bones either from rabbits [20] or rats [13] have been detected.

Several studies have correlated an alteration in mean collagen fibril diameter with bone abnormalities. Morphometric investigations of collagen fibrils of trabecular/cortical bone samples from rear tibia of rabbits and rats in provoked osteoporosis by inflammation or ovariectomy, showed clear differences in comparison with the control groups [13, 20]. Irregular cross-sectional profiles were not detected.

Provoked osteoporosis leads to defects in bone collagen fibril formation and stabilization. Fibril formation is complex and depends on the synthesis of collagenous precursors that undergo numerous secondary or posttranslational modifications which are affected upon osteoporosis as already mentioned. The intermolecular cross-links are responsible for the mechanical strength of collagen, and any reduction will lead to rapid loss of fibril stabilization and, consequently, to decreased mechanical properties of the bone. The possibility that cross-linking during assembly could influence fibril diameters should be

**Table 1** Mean diameter values of female rat and rabbit collagen fibrils from various cortical bone sites [27]

| Animal      | Bone site   | Mean diameter values and SD (nm) |
|-------------|-------------|----------------------------------|
| Normal bone |             |                                  |
| Rat         | Front tibia | 34.5 ± 7.1                       |
| Rat         | Rear tibia  | 38.1 ± 6.5                       |
| Rat         | Femur       | 39.5 ± 6.5                       |
| Rabbit      | Front tibia | 42.7 ± 9.1                       |
| Rabbit      | Rear tibia  | 46.3 ± 8.7                       |
| Rabbit      | Femur       | 43.1 ± 9.9                       |

considered [28]. Cross-linking formation is an extracellular process, and Robey et al. [29] indicated that changes in the functional properties of the extracellular matrix may be involved in osteoporosis. Collagen fibril formation can also be influenced by noncollagenous extracellular matrix components. Many noncollagenous proteins are buried in the extracellular bone matrix from where they can be released when bone is resorbed. Altered concentrations of such proteins in bone matrix [30], or changes in the molecular orientation of these components [31, 32], have been shown to exist in osteoporotic bones.

Trabecular and cortical bone collagen fibril architecture and diameter are affected upon osteoporosis in the same manner. This is very interesting as it has been shown [33] that major collagen type of rat cortical and trabecular bone differs in the extent of posttranslational modifications: the former contains a higher amount of hydroxylysine residues, whereas in the latter, the degree of hydroxylysine glycosylation is higher, and pyridinium cross-link concentration is lower. This would result in fibrils with different mechanical resistance, higher in cortical than in trabecular bone, due to the differing number of structure-stabilizing cross-links.

### 3 Calcium/Phosphorus Ratio Maps of Bone Architecture

Measurements of the Ca/P ratio in different kinds of bones are presented in order to seek information on whether this ratio changes with bone type, site, and abnormalities. This is because, as mentioned in Section 1, the determination of the Ca/P ratio may provide a sensitive measure of bone mineral changes.

It is known that the mechanical strength of bone depends primarily on the condition of the cortical bone [34, 35]. Mechanical testing of excised femoral necks has shown that the cortex contributes 40–60% of the overall strength of the femur [36]. In addition, finite element modeling has suggested that cortical bone in the femoral neck region may support 50% of the stresses associated with normal gait [37]. Hence, in the present review, the presented work regarding bone calcium/phosphorus ratio maps comes only from cortical bone.

#### 3.1 X-Ray Absorptiometry

A new clinical method has been put forward for assessing the skeletal Ca/P ratio in vivo, using photon absorptiometry [23, 38, 39]. The new system uses two photon energies of 39 and 89 KeV obtained by placing cerium and samarium filters in the X-ray beam. It is optimized for measuring the Ca/P ratio at a fixed site in the distal third of the right radius. The method assumes that bone is a three-component system: Ca, PO<sub>4</sub>, and water. This may be a useful measurement to assess bone disorders and age changes, particularly if it can be accomplished noninvasively. In order to evaluate the value of the new method as a diagnostic indicator for bone disorders, the precision and accuracy of the technique must be sufficient to satisfy the requirement for being able to distinguish differences between study populations.

Using this instrument, a significant difference in the mean Ca/P ratio between postmenopausal osteoporotic patients and premenopausal controls has been observed [39]. The mean radius Ca/P ratio in osteoporotic females was 1.29. This Ca/P ratio mean value was significantly lower ( $p < 0.01$ ) than that of 1.71 from normal adult females. From in vitro studies in rabbits, a significant decrease ( $p < 0.01$ ) in the rear tibia Ca/P ratio in animals

with inflammation-mediated osteoporosis (IMO) compared to Ca/P ratio in controls has also been found [23]. The decrease in the Ca/P ratio is suggestive of a major difference in the underlying mechanisms involved in these forms of osteoporosis. As in osteoporotic rabbits, severe structural abnormalities in the rabbit tibia collagen have been detected [20], the same authors suggest that alterations in the Ca/P ratio may be indicative of underlying changes in the organic matrix of bone, mainly in collagen.

An important aspect is the ability of this modified dual X-ray absorptiometry system to choose bone sites, for performing measurements that have a minimum of marrow fat. Marrow fat can be a source of considerable error, as judged by experiments [38] on sheep rear tibia. The Ca/P ratio, as measured by  $\gamma$ -ray absorptiometry, was 1.44, significantly higher ( $p < 0.01$ ) than that obtained after removal of bone marrow, 1.19.

Other workers performing measurements on intact bones by neutron activation analysis have shown that the Ca/P ratio depends upon the kind of bone studied [40–43]. The different values obtained in the different intact bone sites are due to the influence of the organic matrix, i.e., fat, lipids, and marrow (particularly that of red marrow) which depend on bone type [38, 40, 44]. This indicates the importance of selecting suitable animal models when applying results to human studies.

### 3.2 Synchrotron Radiation Microtomography

Synchrotron sources have been shown to provide more accurate assessment of bone mineral content [45–47] as well as providing high resolution, high signal-to-noise ratio imaging [48]. Accurately mapping the linear attenuation coefficient through the use of CT procedures allows different chemical components to be studied throughout the volume of the bone sample [46, 49–51]. MicroCT has been applied successfully to trabecular and cortical bones from humans [45, 46, 48, 52–54], rats [35, 55–57], and mice [58]. One of the major advantages of using a synchrotron source for microCT is the lack of beam hardening effects thus allowing small changes in the attenuation coefficient to be studied throughout the sample.

All measurements presented in this review were performed at the ELETTRA Synchrotron Light Laboratory in Trieste, Italy. MicroCT data sets were collected using the CT set-up on the SYRMEP (synchrotron radiation for medical physics) beamline. This set-up consists of a high precision rotary table mounted upon high accuracy translators and cradles. This allows precise alignment of the rotation axis of the sample with the detector pixels. A full data set consisted of 360 views over  $180^\circ$ , and for each sample, data were collected at 20 keV. It has been shown [24, 39, 40] that calcium phosphate bone substitutes can be used to accurately represent bone with different Ca/P ratios. Thus, two calibration phantoms, as bone substitutes, were also imaged. Multiple 2D slices were reconstructed from the 3D data sets with a slice thickness of  $\sim 28 \mu\text{m}$ . A full data set typically contained 140 slices. For the analysis, all CT values were converted to Ca/P values using the calibration phantom results.

Table 2 summarizes the results from the analysis of the bulk Ca/P ratios. Samples were taken from different experimental animals and different locations [59]. Statistically significant differences ( $p < 0.001$ ) were detected in Ca/P ratios in different bone sites from different experimental animals [59, 60]. For example, in rabbits, the mean Ca/P value for cortical femur is  $1.28 \pm 0.21$ , while for cortical rear tibia,  $1.75 \pm 0.08$ . It is worth noting that while in rats the mean Ca/P value for cortical femur is significantly greater ( $p < 0.001$ ) than that of rear tibia, in rabbits, the greatest mean value is that for the rear tibia. In addition, the

**Table 2** Bulk Ca/P ratio values from cortical bone samples [59]

| Group/animal          | Bone site   | Bulk Ca/P ratio |
|-----------------------|-------------|-----------------|
| Normal bone           |             |                 |
| Lamb                  | Rear tibia  | 1.35 ± 0.17     |
| Rabbit                | Rear tibia  | 1.75 ± 0.08     |
| Rabbit                | Femur       | 1.28 ± 0.21     |
| Rat                   | Femur       | 2.12 ± 0.08     |
| Rat                   | Front tibia | 1.75 ± 0.06     |
| Rat                   | Rear tibia  | 1.94 ± 0.07     |
| Osteoporotic bone-IMO |             |                 |
| Rabbit                | Rear tibia  | 1.47 ± 0.07     |

Ca/P ratio in the same bone site from different species has a significant variation. In lamb, rabbit, and rat cortical rear tibia, the corresponding mean Ca/P values are:  $1.35 \pm 0.17$ ,  $1.75 \pm 0.08$ , and  $1.94 \pm 0.07$  [Table 2]. Different life activities arising from the evolutionary adaptation of these species could be considered as a possible explanation for the observed variation. Lambs have been adapted for walking and rabbits for jumping, while rats have been adapted for running. These movement activities exert differing pressure conditions on their front and rear legs, and as a consequence, their bone strength has to be respectively adapted. The Ca/P ratio could easily be one of these adaptations.

The variations with different animals and bone sites obtained with microCT support the view of the necessity of careful selection of experimental models when applying results to humans.

In addition, the findings listed in Table 2 show a significant difference ( $p < 0.001$ ) in Ca/P ratios between osteoporotic versus normal bone similar to that obtained by using X-ray absorptiometry, suggesting that there is a relationship between bone loss and a lowered Ca/P ratio.

### 3.3 Collagen Fibril Diameter in Relation to Calcium/Phosphorus Ratio

Measurements of collagen fibril diameter in cortical bone samples from the femoral neck, rear and front tibia of rabbits and rats showed that, in rats, the greatest mean diameter value is that for the femur, while for rabbits is that for the rear tibia. Furthermore, in both experimental animals, the smallest mean value is that for the front tibia [27]. An important aspect is the agreement between these observations and the mean values for Ca/P ratio, mentioned above.

It appears that there exists a relationship between collagen fibril diameter and the Ca/P ratio for the same kind of experimental animal and bone site. Both of these parameters can be used as indexes of bone quality [23]. As has been reported [40–42], the Ca/P ratio may provide high reliability for the diagnosis, prevention, and treatment of bone disorders. In addition, alterations in the skeletal Ca/P ratio with disease may be indicative of underlying changes in the organic matrix of bone, mainly collagen [23]. Also, lines of evidence suggest that there is a relationship between osteoporosis and alterations in the bone Ca/P ratio [23, 39, 51] and in bone collagen fibril diameter [13, 20]. As bone Ca/P ratio and collagen fibril diameter decline in parallel upon osteoporosis, the present observations may have a significant input in understanding the pathogenesis of some of the most troublesome, painful bone disorders that afflict mankind.

## 4 Conclusions

The skeletal Ca/P ratio has been shown to be a good index of bone quality. In addition, results presented here also confirm that there is a relationship between bone loss and a lowered Ca/P ratio. As nowadays we can measure bone Ca/P ratio in vivo for use as a clinical indicator [38, 39], such measurements could also be useful for the treatment of the bone diseases in which, along with bone loss, the bone quality is affected. It has previously been shown [61] that, in ovariectomized rats, the structural alterations in bone collagen initiated by the loss of ovarian hormones are much less severe upon appropriate treatment.

The overall socioeconomic benefit derived from early diagnosis and prevention of bone disorders is important because it improves the quality of life of a large number of patients and minimizes the cost of treating the severe disabilities caused by these diseases. Since a great number of people are susceptible to bone disorders, effective diagnostic techniques and prevention is in crucial demand. This review provides evidence that both X-ray absorptiometry and microtomography can be used to reliably measure the Ca/P of bone in both humans and experimental animals and, hence, could be valuable techniques to be used during bone therapeutic and diagnostic trials.

## References

- Kaplan, F.S., Hayes, W.C., Keaveny, T.M., Boskey, A., Einhorn, J.P., Iannotti, J.P.: Form and function of bone. In: Simon, S.R., (ed.) *Orthopaedic Basic Science*, pp. 127–184. American Academy of Orthopaedic Surgeons, Rosemont, IL (1994)
- Rubin, M.A., Rubin, J., Jasiuk, I.: SEM and TEM study of the hierarchical structure of C57BL/6J and C3H/HeJ mice trabecular bone. *Bone* **35**, 1–20 (2004). doi:[10.1016/j.bone.2004.02.008](https://doi.org/10.1016/j.bone.2004.02.008)
- Kjaer, M.: Role of extracellular matrix in adaptation of tendon and skeletal muscle to mechanical loading. *Physiol. Rev.* **84**, 649–698 (2004). doi:[10.1152/physrev.00031.2003](https://doi.org/10.1152/physrev.00031.2003)
- Dahl, T., Veis, A.: Electrostatic interactions lead to the formation of asymmetric collagen-phosphoryn aggregates. *Connect. Tissue Res.* **44**(Suppl 1), 206–213 (2003). doi:[10.1080/713713589](https://doi.org/10.1080/713713589)
- Paschalis, E.P., Recker, R., Dicarolo, E., Doty, S.B., Atti, E., Boskey, A.L.: Distribution of collagen cross-links in normal human trabecular bone. *J. Bone Miner. Res.* **18**, 1942–1946 (2003). doi:[10.1359/jbmr.2003.18.11.1942](https://doi.org/10.1359/jbmr.2003.18.11.1942)
- Wu, T.J., Huang, H.H., Lan, C.W., Lin, C.H., Hsu, F.Y., Wang, Y.J.: Studies on the microspheres comprised of reconstituted collagen and hydroxyapatite. *Biomaterials* **25**, 651–658 (2004). doi:[10.1016/S0142-9612\(03\)00576-3](https://doi.org/10.1016/S0142-9612(03)00576-3)
- Midura, R.J., Vasanji, A., Su, X., Wang, A., Midura, S.B., Gorski, J.P.: Calcospherulites isolated from the mineralization front of bone induce the mineralization of type I collagen. *Bone* **41**, 1005–1016 (2007). doi:[10.1016/j.bone.2007.08.036](https://doi.org/10.1016/j.bone.2007.08.036)
- Tzaphlidou, M.: The role of collagen in bone structure: an image processing approach. *Micron* **36**, 593–601 (2005). doi:[10.1016/j.micron.2005.05.009](https://doi.org/10.1016/j.micron.2005.05.009)
- Dalle Carbonare, L., Giannini, S.: Bone microarchitecture as an important determination of bone strength. *J. Endocrinol. Invest.* **27**, 99–105 (2004)
- Mosekilde, L.: Age-related changes in bone mass, structure, and strength—effects of loading. *Z. Rheumatol.* **59**(Suppl 1), 1–9 (2000). doi:[10.1007/s003930070031](https://doi.org/10.1007/s003930070031)
- Akesson, K., Grynpas, M.D., Hancock, R.G.V., Odelius, R., Obrant, K.J.: Energy-dispersive X-ray microanalysis of the bone mineral content in human trabecular bone: a comparison with ICPES and neutron activation analysis. *Calcif. Tissue Int.* **55**, 236–239 (1994). doi:[10.1007/BF00425881](https://doi.org/10.1007/BF00425881)
- Bailey, A.J., Wotton, S.F., Sims, T.J., Thompson, P.W.: Post-translational modifications in the collagen of human osteoporotic femoral head. *Biochem. Biophys. Res. Commun.* **185**, 801–805 (1992). doi:[10.1016/0006-291X\(92\)91697-0](https://doi.org/10.1016/0006-291X(92)91697-0)
- Kafantari, H., Kounadi, E., Fatouros, M., Milonakis, M., Tzaphlidou, M.: Structural alterations in rat skin and bone collagen fibrils induced by ovariectomy. *Bone* **26**, 349–353 (2000). doi:[10.1016/S8756-3282\(99\)00279-3](https://doi.org/10.1016/S8756-3282(99)00279-3)



14. Pace, J.M., Atkinson, M., Willing, M.C., Wallis, G., Byers, P.H.: Deletions and duplications of Gly-Xaa-Yaa triplet repeats in the triple helical domains of type I collagen chains disrupt helix formation and result in several types of osteogenesis imperfecta. *Hum. Mutat.* **18**, 319–326 (2001). doi:[10.1002/humu.1193](https://doi.org/10.1002/humu.1193)
15. Batge, B., Diebold, J., Stein, H., Bodo, M., Muller, P.K.: Compositional analysis of the collagenous bone matrix—a study on adult normal and osteopenic bone tissue. *Eur. J. Clin. Invest.* **22**, 805–812 (1992). doi:[10.1111/j.1365-2362.1992.tb01450.x](https://doi.org/10.1111/j.1365-2362.1992.tb01450.x)
16. Bank, R.A., Tekopelle, J.M., Janus, G.J., Wassen, M.H., Pruijs, H.E., Van der Sluijs, H.A., Sakkars, R.J.: Pyridinium cross-links in bone of patients with osteogenesis imperfecta: evidence of a normal intrafibrillar collagen packing. *J. Bone Miner. Res.* **15**, 1330–1336 (2000). doi:[10.1359/jbmr.2000.15.7.1330](https://doi.org/10.1359/jbmr.2000.15.7.1330)
17. Prockop, D.J., Constantinou, C.D., Dombrowski, K.E., Hojima, Y., Kadler, K.E., Kuivaniemi, H., Tromp, G., Vogel, B.E.: Type I procollagen: the gene–protein system that harbors most of the mutations causing osteogenesis imperfecta and probably more common heritable disorders of connective tissue. *Am. J. Med. Genet.* **34**, 60–67 (1989). doi:[10.1002/ajmg.1320340112](https://doi.org/10.1002/ajmg.1320340112)
18. Rubin, M.A., Jasiuk, I., Taylor, J., Rubin, J., Ganey, T., Apkarian, R.P.: TEM analysis of the nanostructure of normal and osteoporotic human trabecular bone. *Bone* **33**, 270–282 (2003). doi:[10.1016/S8756-3282\(03\)00194-7](https://doi.org/10.1016/S8756-3282(03)00194-7)
19. Adachi, E., Hopkinson, I., Hayashi, T.: Basement–membrane stromal relationships: interactions between collagen fibrils and the lamina densa. *Int. Rev. Cytol.* **173**, 73–156 (1997). doi:[10.1016/S0074-7696\(08\)2476-6](https://doi.org/10.1016/S0074-7696(08)2476-6)
20. Kounadi, E., Fountos, G., Tzaphlidou, M.: The influence of inflammation-mediated osteopenia (IMO) on the structure of rabbit bone and skin collagen fibrils. *Connect. Tissue Res.* **37**, 69–76 (1998). doi:[10.3109/03008209809028901](https://doi.org/10.3109/03008209809028901)
21. Tzaphlidou, M., Kounadi, E., Kafantari, H.: Influence of lithium on mouse bone collagen fibrils. *J. Trace Microprobe Tech.* **18**, 321–326 (2000)
22. Diebold, J., Batge, B., Stein, H., Muller-Esch, G., Muller, P.K., Lohrs, U.: Osteoporosis in longstanding acromegaly: characteristic changes of vertebral trabecular architecture and bone matrix composition. *Virchows Arch., A Pathol. Anat. Histopathol.* **419**, 209–215 (1991). doi:[10.1007/BF01626350](https://doi.org/10.1007/BF01626350)
23. Fountos, G., Kounadi, E., Tzaphlidou, M., Yasumura, S., Glaros, D.: The effects of inflammation-mediated osteoporosis (IMO) on the skeletal Ca/P ratio and on the structure of rabbit bone and skin collagen. *Appl. Radiat. Isotopes* **49**, 657–659 (1998). doi:[10.1016/S0969-8043\(97\)00086-9](https://doi.org/10.1016/S0969-8043(97)00086-9)
24. Parry, D.A., Barnes, G.R., Craig, A.S.: A comparison of the size distribution of collagen fibrils in connective tissues as a function of age and a possible relation between fibril size distribution and mechanical properties. *Proc. R. Soc. Lond. B* **203**, 305–321 (1978)
25. Baek, G.H., Carlin, G.J., Vogrin, T.M., Woo, S.L., Harner, C.D.: Quantitative analysis of collagen fibrils of human cruciate and meniscofemoral ligaments. *Clin. Orthop. Relat. Res.* **357**, 205–211 (1998). doi:[10.1097/00003086-199812000-00026](https://doi.org/10.1097/00003086-199812000-00026)
26. Ottani, V., Franchi, M., De Pasquale, V., Leonardi, L., Morocutti, M., Ruggeri, A.: Collagen fibril arrangement and size distribution in monkey oral mucosa. *J. Anat.* **192**, 321–328 (1998). doi:[10.1046/j.1469-7580.1998.19230321.x](https://doi.org/10.1046/j.1469-7580.1998.19230321.x)
27. Berillis, P., Emfietzoglou, D., Tzaphlidou, M.: Collagen fibril diameter in relation to bone site and to calcium/phosphorus ratio. *Sci. World J.* **6**, 1109–1113 (2006). doi:[10.1002/isw.2006.212](https://doi.org/10.1002/isw.2006.212) doi:[10.1100/tsw.2006.212](https://doi.org/10.1100/tsw.2006.212)
28. Chapman, J.A.: Molecular organisation in the collagen fibril. In: Hukins, D.W.L. (ed.) *Connective Tissue Matrix*, pp. 89–132. Verlag Chemie (1984)
29. Robey, P.G., Fedarko, N.S., Hefferan, T.E., Bianco, P., Vetter, U.K., Grzesik, W., Friedenstein, A., Van Der Pluijm, G., Mintz, K.P., Young, M.F., Kerr, J.M., Ibaraki, K., Heegard, A.M.: Structure and molecular of bone matrix proteins. *J. Bone Miner. Res.* **8**, 483–487 (1993)
30. Aerssens, J., Dequeker, J., Mbuyi-Muamba, J.M.: Bone tissue composition: biochemical anatomy of bone. *Clin. Rheumatol.* **13**, 54–62 (1994). doi:[10.1007/BF02229866](https://doi.org/10.1007/BF02229866)
31. Ferris, B.D., Klenerman, L., Dodds, R.A., Bitensky, L., Chayen, J.: Altered organization of non-collagenous bone matrix in osteoporosis. *Bone* **8**, 285–288 (1987). doi:[10.1016/8756-3282\(87\)90003-2](https://doi.org/10.1016/8756-3282(87)90003-2)
32. Kent, G.N., Dodds, R.A., Bitensky, L., Klenerman, L., Watts, R.W.E., Chayen, J.: Changes in crystal size and orientation of acidic glycosaminoglycans at the fracture site in fractured necks of femur. *J. Bone Jt. Surg.* **65-B**, 189–194 (1983)
33. Suarez, K.N., Romanello, M., Bettica, P., Moro, L.: Collagen type I of rat cortical and trabecular bone differs in the extent of posttranslational modifications. *Calcif. Tissue Int.* **58**, 65–69 (1996). doi:[10.1007/BF02509548](https://doi.org/10.1007/BF02509548)
34. Stein, I.D., Granik, G.: Rib structure and bending strength: an autopsy study. *Calcif. Tissue Res.* **20**, 61–73 (1976). doi:[10.1007/BF02546398](https://doi.org/10.1007/BF02546398)

35. Stenstrom, M., Olander, B., Lehto-Axtelius, D., Madsen, J.E., Nordsletten, L., Carlsson, G.A.: Bone mineral density and bone structure parameters as predictors of bone strength: an analysis using computerized microtomography and gastrectomy-induced osteopenia in the rat. *J. Biomech.* **33**, 289–297 (2000). doi:[10.1016/S0021-9290\(99\)00181-5](https://doi.org/10.1016/S0021-9290(99)00181-5)
36. Werner, C., Iversen, B.F., Therkildsen, M.H.: Contribution of the trabecular component to mechanical strength and bone mineral content of the femoral neck. An experimental study on cadaver bones. *Scand. J. Clin. Lab. Invest.* **48**, 457–460 (1988). doi:[10.3109/00365518809085757](https://doi.org/10.3109/00365518809085757)
37. Lotz, J.C., Cheal, E.J., Hayes, W.C.: Stress distributions within the proximal femur during gait and falls: implications for osteoporotic fracture. *Osteoporos. Int.* **5**, 252–261 (1995). doi:[10.1007/BF01774015](https://doi.org/10.1007/BF01774015)
38. Fountos, G., Yasumura, S., Glaros, D.: The skeletal calcium/phosphorus ratio: a new in vivo method of determination. *Med. Phys.* **24**, 1303–1310 (1997). doi:[10.1118/1.598152](https://doi.org/10.1118/1.598152)
39. Fountos, G., Tzaphlidou, M., Kounadi, E., Glaros, D.: In vivo measurement of radius calcium/phosphorus ratio by X-ray absorptiometry. *Appl. Radiat. Isotopes* **51**, 273–278 (1999). doi:[10.1016/S0969-8043\(99\)00056-1](https://doi.org/10.1016/S0969-8043(99)00056-1)
40. Tzaphlidou, M., Zaichick, V.: Neutron activation analysis of calcium/phosphorus ratio in rib bone of healthy humans. *Appl. Radiat. Isotopes* **57**, 779–783 (2002). doi:[10.1016/S0969-8043\(02\)00171-9](https://doi.org/10.1016/S0969-8043(02)00171-9)
41. Tzaphlidou, M., Zaichick, V.: Calcium, phosphorus, calcium–phosphorus ratio in rib bone of healthy humans. *Biol. Trace Elem. Res.* **93**, 63–74 (2003). doi:[10.1385/BTER:93:1-3:63](https://doi.org/10.1385/BTER:93:1-3:63)
42. Zaichick, V., Tzaphlidou, M.: Determination of calcium, phosphorus, and the calcium/phosphorus ratio in cortical bone from the human femoral neck by neutron activation analysis. *Appl. Radiat. Isotopes* **56**, 781–786 (2002). doi:[10.1016/S0969-8043\(02\)00066-0](https://doi.org/10.1016/S0969-8043(02)00066-0)
43. Zaichick, V., Tzaphlidou, M.: Calcium and phosphorus concentrations and the calcium/phosphorus ratio in trabecular bone from the femoral neck of healthy humans as determined by neutron activation analysis. *Appl. Radiat. Isotopes* **58**, 623–627 (2003). doi:[10.1016/S0969-8043\(03\)00092-7](https://doi.org/10.1016/S0969-8043(03)00092-7)
44. Bolotin, H.H., Sievanen, H.: Inaccuracies inherent in dual-energy X-ray absorptiometry in vivo bone mineral density can seriously mislead diagnostic/prognostic interpretations of patient-specific bone fragility. *J. Bone Miner. Res.* **16**, 799–805 (2001). doi:[10.1359/jbmr.2001.16.5.799](https://doi.org/10.1359/jbmr.2001.16.5.799)
45. Peyrin, F., Salome, M., Nuzzo, S., Cloetens, P., Laval-Jeantet, A.M., Baruchel, J.: Perspectives in three-dimensional analysis of bone samples using synchrotron radiation microtomography. *Cell. Mol. Biol.* **46**, 1089–1102 (2000)
46. Nuzzo, S., Peyrin, F., Cloetens, P., Baruchel, J., Boivin, G.: Quantification of the degree of mineralization of bone in three dimensions using synchrotron radiation microtomography. *Med. Phys.* **29**, 2672–2681 (2002). doi:[10.1118/1.1513161](https://doi.org/10.1118/1.1513161)
47. Postnov, A.A., Vinogradov, A.V., Van Dyck, D., Saveliev, S.V., De Clerck, N.M.: Quantitative analysis of bone mineral content by X-ray microtomography. *Physiol. Meas.* **24**, 165–178 (2003). doi:[10.1088/0967-3334/24/1/312](https://doi.org/10.1088/0967-3334/24/1/312)
48. Salome, M., Peyrin, F., Cloetens, P., Odet, C., Laval-Jeante, A.M., Baruchel, J., Spanne, P.: A synchrotron radiation microtomography system for the analysis of trabecular bone samples. *Med. Phys.* **26**, 2194–2204 (1999). doi:[10.1118/1.598736](https://doi.org/10.1118/1.598736)
49. Davis, G.R., Wong, F.S.: X-ray microtomography of bones and teeth. *Physiol. Meas.* **17**, 121–146 (1996). doi:[10.1088/0967-3334/17/3/001](https://doi.org/10.1088/0967-3334/17/3/001)
50. Kinney, J.H., Haupt, D.L., Balooch, M., Ladd, A.J., Lane, N.E.: Three-dimensional morphometry of the L6 vertebra in the ovariectomized rat model of osteoporosis: biomechanical implications. *J. Bone Miner. Res.* **15**, 1981–1991 (2000). doi:[10.1359/jbmr.2000.15.10.1981](https://doi.org/10.1359/jbmr.2000.15.10.1981)
51. Tzaphlidou, M., Speller, R., Royle, G., Griffiths, J., Olivo, A., Pani, S., Longo, R.: High resolution Ca/P maps of bone architecture in 3D synchrotron radiation microtomographic images. *Appl. Radiat. Isotopes* **62**, 569–575 (2005). doi:[10.1016/j.apradiso.2004.10.003](https://doi.org/10.1016/j.apradiso.2004.10.003)
52. Nuzzo, S., Lafage-Proust, M.H., Martin-Badosa, E., Boivin, G., Thomas, T., Alexandre, C., Peyrin, F.: Synchrotron radiation microtomography allows the analysis three-dimensional microarchitecture and degree of mineralization of human iliac crest biopsy specimens: effects etidronate treatment. *J. Bone Miner. Res.* **17**, 1372–1382 (2002). doi:[10.1359/jbmr.2002.17.8.1372](https://doi.org/10.1359/jbmr.2002.17.8.1372)
53. Nuzzo, S., Meneghini, C., Brailion, P., Bouvier, R., Mobilio, S., Peyri, F.: Microarchitectural and physical changes during fetal growth in human vertebral bone. *J. Bone Miner. Res.* **18**, 760–768 (2003). doi:[10.1359/jbmr.2003.18.4.760](https://doi.org/10.1359/jbmr.2003.18.4.760)
54. Bousson, V., Peyrin, F., Bergot, C., Hausard, M., Sautet, A., Laredo, J.D.: Cortical bone in the human femoral neck: three-dimensional appearance and porosity using synchrotron radiation. *J. Bone Miner. Res.* **19**, 794–802 (2004). doi:[10.1359/JBMR.040124](https://doi.org/10.1359/JBMR.040124)
55. Stenstrom, M., Olander, B., Carlsson, C.A., Carlsson, G.A., Lehto-Axtelius, D., Hakanson, R.: The use of computed microtomography to monitor morphological changes in small animals. *Appl. Radiat. Isotopes* **49**, 565–570 (1998). doi:[10.1016/S0969-8043\(97\)00189-9](https://doi.org/10.1016/S0969-8043(97)00189-9)

56. Barbier, A., Martel, C., de Vernejoul, M.C., Tirode, F., Nys, M., Mocaer, G., Morieux, C., Murakami, H., Lacheretz, F.: The visualization and evaluation of bone architecture in the rat using three-dimensional X-ray microcomputed tomography. *J. Bone Miner. Metab.* **17**, 37–44 (1999). doi:[10.1007/s007740050061](https://doi.org/10.1007/s007740050061)
57. Laib, A., Barou, O., Vico, L., Lafage-Proust, M.H., Alexandre, C., Ruegsegger, P.: 3D micro-computed tomography of trabecular and cortical bone architecture with application to a rat model of immobilisation osteoporosis. *Med. Biol. Eng. Comput.* **38**, 326–332 (2000). doi:[10.1007/BF02347054](https://doi.org/10.1007/BF02347054)
58. Martin-Badosa, E., Elmoutaouakkil, A., Nuzzo, S., Amblard, D., Vico, L., Peyrin, F.: A method for the automatic characterization of bone architecture in 3D mice microtomographic images. *Comput. Med. Imaging Graph.* **27**, 447–458 (2003). doi:[10.1016/S0895-6111\(03\)00031-4](https://doi.org/10.1016/S0895-6111(03)00031-4)
59. Speller, R., Pani, S., Tzaphlidou, M., Horrocks, J.: MicroCT analysis of calcium/phosphorus ratio maps at different bone sites. *Phys. Res. A* **548**, 269–273 (2005)
60. Tzaphlidou, M., Speller, R., Royle, G., Griffiths, J.: Preliminary estimates of the calcium/phosphorus ratio at different cortical bone sites using synchrotron microCT. *Phys. Med. Biol.* **51**, 1849–1855 (2006). doi:[10.1088/0031-9155/51/7/015](https://doi.org/10.1088/0031-9155/51/7/015)
61. Tzaphlidou, M., Kafantari, H.: Influence of nutritional factors on bone collagen fibrils in ovariectomized rats. *Bone* **27**, 635–638 (2000). doi:[10.1016/S8756-3282\(00\)00382-3](https://doi.org/10.1016/S8756-3282(00)00382-3)